A PHYSICOCHEMICAL ASSESSMENT OF UPPER CATCHMENT WITHIN THE AYER HITAM FOREST RESERVE, PENINSULAR MALAYSIA

NURHIDAYU SITI[1]*, NORDIN SITI FATIMAH [1], SULAIMAN MOHD SOFIYAN[2,3], MOHAMAD KASSIM MOHAMAD ROSLAN [1] AND SANG YAN-FANG[4]

[1]*Faculty of Forestry and Environment, Universiti Putra Malaysia, 43400 UPM Serdang, Selangor, Malaysia.* [2]*Faculty of Ocean Engineering Technology and Informatics,* [3]*Hydrology and Water Resources Research Interest Group, Universiti Malaysia Terengganu, 21030 Kuala Nerus, Terengganu, Malaysia.* [4]*Key Laboratory of Water Cycle and Related Land Surface Processes, Institute of Geographic Sciences and Natural Resources Research, Chinese Academy of Sciences, Beijing 100101, China.*

*Corresponding author: sitinurhidayu@upm.edu.my

Abstract: Isolated forests located in rapidly developing areas play a crucial role in providing water resources, regulating climate, filtering water pollution, and mitigating flood events. The Ayer Hitam Forest Reserve (AHFR) is one of the most precious tracts of the remaining lowland dipterocarp forest in the highly urbanized state of Selangor, Malaysia. Until recently, there have been no comprehensive datasets available on hydrological data in AHFR. This study aims to assess the seasonal physicochemical characteristics from a matured secondary catchment forest in AHFR, which is surrounded by the metropolitan city of the Klang Valley. Its physical characteristics are denoted by streamflow, turbidity, and Total Suspended Solids (TSS). The chemical characteristics consist of dissolved oxygen (DO), temperature, pH, Electrical Conductivity (EC), salinity, and Total Dissolved Solids (TDS). The results indicated that the baseflow discharges ranged from 0.020 to 0.680 m^3/s, while stormflow discharges ranged from 0.003 to 1.090 m^3/s. Only pH and TSS are categorized under Class 3 during storm events. The findings implied that a catchment was capable of recharging the baseflow during low rainfall periods and producing high-quality water, which is important to safeguard the water resources and hydrological functions of a catchment within an isolated forest.

Keywords: Isolated forest, physicochemical, water quality, river discharge, hydro-environment.

Introduction

Over the past 50 years, the global population has grown more rapidly than any other time in history which places high pressure on demand for water resources. The United Nations (2011) assumes that by 2050, the estimated population could increase to more than nine billion based on an increase from 2.5 billion people in 1950 to 6.6 billion people in 2010. Grimm *et al.* (2008) expects the percentage of the global population living in cities to reach 60% by 2030, in which the research was based on the 40% expansion from the 1990 to 2008. Most of the population increase occurred in tropical regions of developing cities (United Nations, 2011). Urbanization, along with a rapidly growing population, forest conversion, unsustainable water use, industrial development, and climate change, have pressured people into prioritizing the quality and quantity aspects of the natural system, thus endangering water security (Ceola *et al.*, 2015; Xiao-Jun *et al.,* 2015).

Southeast Asia covers almost 11% of the world's tropical forest area and has the highest deforestation rate among tropical areas (Houghton & Hackler, 1999; Laurance, 1999; Malhi & Grace, 2000; Canadell *et al.*, 2007). Half of Asian nations have experienced severe (> 70%) forest loss. Forest-rich countries, such as Indonesia and Malaysia, are experiencing rapid forest destruction (Laurance, 2007). A study at the Kelantan River Basin (KRB), Malaysia, revealed that land-use modifications through intensive deforestation for urban and agriculture establishments have induced

localized climate variability and hydrological patterns in the KRB, causing an upsurge of disaster severity (Faizalhakim *et al.,* 2017). Consequently, deforestation impacts global and regional climate change, as well as hydrologic cycling (Kanae *et al.*, 2001; Malhi & Wright, 2004; Mabuchi *et al.*, 2005; Werth & Avissar, 2005).

Forests in the tropical regions still experience a high level of degradation and remain poorly protected (Sodhi *et al.*, 2004; Lawson, 2015). One of the major constituents of deforestation is unsustainable timber production. Timber production usually poses a significant threat to forest ecosystems, especially in tropical regions. Department of Statistics Malaysia (2005) revealed that the total forest area in Peninsular Malaysia is 5.94 million hectares, representing 45.2% of the total land-use area. The total forest land-use area includes forest areas allocated for timber concessions. Replanting various species of trees approved by the Forestry Department of Peninsular Malaysia begins once harvesting operations end (Rahim & Shahwahid, 2009). Linear infrastructure, such as roads, highways, gas lines, and power lines, are omnipresent features of human activity and rapidly spreading in the tropics, enhancing forest opening (Laurance *et al.*, 2009).

The availability of water resources is crucial to provide adequate water supply in conjunction with an increasing population and its economic development. In the future, conflicts related to catchment areas will pressure societal demands for water. Threats to catchment areas targeted for development purposes will lead to future water supply depreciation due to intensified demands for water resources (Syuhada *et al.*, 2018). Water consumption has increased throughout decades of civilization, as is evident from the increase of the freshwater withdrawal rate from 1.589 km³/d in 1900 to 3.742 km³/d in 1950 and subsequently to 10.416 km³/d as of 2000 (Peter, 2000). Concern for insufficient freshwater resources in the future has forced developing countries to assess river water quality and quantity in recent years.

Forest conversion causes serious impacts on biodiversity, including population decline, species extinction, and the alteration of ecological processes (Morante-Filho *et al*., 2018). Deforestation and fragmentation erode biodiversity by reducing effective habitat areas and quality, increasing its exposure to disturbance (Deere *et al.*, 2020). Deep roots are generally considered an efficient way of adaptation to drought in tropical and subtropical forests (Yang *et al.,* 2015). Fast downward growth of roots provides access to large amounts of water stored in deep soil layers after wet seasons, buffering the intra-annual variability of rainfall distribution, and sustaining tree growth over the following dry periods (Christina *et al.,* 2017).

Thus, the increasing global population, degradation of tropical forests, and inadequate water supply were the premises for the initiation of research at a secondary tropical forest catchment in Klang Valley, Malaysia. The Ayer Hitam Forest Reserve (AHFR) was selected for a case study due to its significant location within the city and potential storage of water resources during storm events. The existence of a forest patch at AHFR provides water security to the main river downstream. The contributions of baseflow and water retention by AHFR during storm events are of main importance for the city's overall landscape. This study aims to assess seasonal physicochemical characteristics from a matured secondary forest catchment concerning the conservation of the isolated forest catchment as a water resource with a definite water quality status. The relationship between a storm event and the physicochemical characteristics of water was elucidated using correlation analysis, cluster analysis, and principal component analysis to better understand the trend and variation of water quality at AHFR.

Materials and Methods

Description of Study Area

Observations were conducted within 4.66 km^2 of matured secondary forest catchment located within the isolated AHFR in the Klang Valley, Selangor (see Figure 1a). The AHFR has appointed the Faculty of Forestry, Universiti Putra Malaysia, to conduct research. Education activity started from 1996 until the end of the concession year (2076). The increasing population has put pressure on the forest catchment, creating a high demand for development within its vicinity. There are only two main streams in AHFR: the Bohol River and the Rasau River (Hasmadi & AL, 2017). The catchment outlet is situated at N 03°00′55.8 and E 101°38′53.5 on the Rasau River. Figure 1b displays the outlet point located at approximately 3 m before reaching the waterfall known as the 'blue lagoon', otherwise named as the Upper Rasau catchment. The study site was mainly covered with disturbing trees composed of Kelat–Kedondong–Mixed Dipterocarp lowland forest species (Faridah-Hanum & Rosly, 2000). The site elevation was within 15 m to 208 m
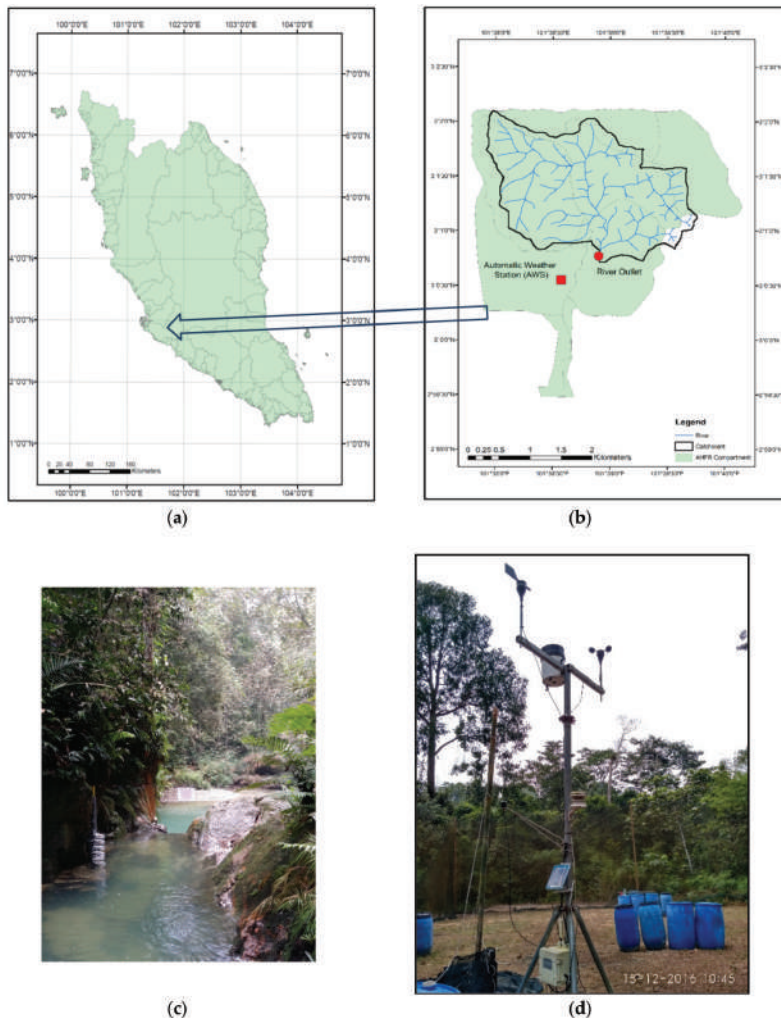

Figure 1: Location of the Upper Rasau catchment within: (a) Peninsular Malaysia; (b) Ayer Hitam Forest Reserve (AHFR); (c) the automatic water level sensor and manual stage board for water level monitoring installed at the catchment outlet; and (d) the weather station at AHFR

from the mean sea level, with the highest peak located at the Permatang Kuang.

This area has become an important conservation area, as it is considered the most massive patch of forest in the Klang Valley. The soil types in the forests are the Serdang–Bungor series and Serdang–Kedah series, which are derived from sedimentary and metamorphic rocks (Wong, 1970; Bawon, 2007). The Serdang soil series character undulates and rolls to hilly lands, while shallow soils of Kedah series sit on steeper terrain. The parent materials are composed of quartzites, sandstones, and sandy shale with intercalations of micaceous, silty shale, and phyllites. This makes the colors of these soils vary from dark brown to tones of greyish-brown or yellowish-brown, with a pH of 5 (Neto *et al.*, 2012). The soil along the hills and ridges consists of local alluvium and colluvium, which results from mixing sandy clay loam soil with metamorphic rock originated from the upper areas (Lai & Samsuddin, 1985; Neto *et al.*, 2012).

The forest area originally spanned to 4270.7 ha in 1906 and shrank to 1248 ha in 2008 due to rapid development for residential and industrial uses (Hasmadi & AL, 2017). From 1936 - 1984, the Forestry Department of Malaysia applied selective logging under the Malayan Uniform System (MUS). The crawler tractor-Santai Wong system, in which A-16 Komatsu was used to transfer the extracted log, had resulted in logging roads in AHFR (Lai & Samsuddin, 1985). Until present, the previous logging road has been utilized as accessible routes within the forest area. The density of roads within the catchment area was 0.512 km/km². Later in 2008, 3702.5 m² in Compartment 15 was developed into a center of improvement for learning and research activities (Norizah *et al.*, 2014).

The climate of Peninsular Malaysia is tropical and affected by the SW and NE monsoons. It is characterized by uniform temperature throughout the year, specifically light winds and high humidity. The monthly mean temperature in Kuala Lumpur varies less than 2°C a year, but the daily variation is approximately 10°C.

From 1992–2009, Pusat Pertanian Serdang (3° 00′ N, 101° 42′ E, 44 m asl) had registered 2557 mm of average annual rainfall over 16 years, compared to 206 rainy days, 94% of average relative humidity (eight years), and an average temperature of 24°C at 8 a.m. (nine years). From 1985 - 2004, the Malaysian Agricultural Research and Development Institute (MARDI) in Serdang (2° 59′ N, 101° 40′ E, 38 m asl) had 2463 mm of average annual rainfall (20 years), corresponding to 191 rainy days, 24°C of average temperature (19 years), and 96% of average relative humidity at 8 a.m. (eight years). These stations are 6 and 4 km away, respectively, from AHFR towards S–SE (MMD 2010). Rainfall in the west has two maxima in April and between October–November, as well as two minima in February and July (Neto *et al.*, 2012).

The experimental catchment took up nearly 40% of the total area of AHFR. The catchment outlet was selected based on the stable physical features located about 2 m before the 'blue lagoon' waterfall for stable water level measurement. The catchment outlet was also determined considering that the contributing area into rivers was located on the upstream of the outlet without used forest land. The catchment boundary was delineated in ArcGIS 10.3 using digital elevation model (DEM) data and shuttle radar topography mission (SRTM) 30 m from USGS Earth Explorer. The area and other catchment characteristics were determined using ArcGIS 10.3 (Table 1).

Table 1: Characteristics of the Upper Rasau catchment within the Ayer Hitam Forest Reserve (AHFR)

Measures	Value
Area (km²)	4.66
Perimeter (km)	20.17
Range of elevation (m)	28.52–242.79
Slope range (°)	0.1–64.6
River length (km)	22.65
Drainage density (km/km²)	4.86
Stream order (Strahler method)	5
Length of the watershed (km)	2.53
Channel gradient (%)	3.29

Climate Data

The automatic weather station (AWS) in the AHFR was installed in March 2015 to monitor rainfall density, rain days, temperature, and relative humidity. The location of AWS is shown in Figure 1c. Data on an hourly basis were transferred using the Universal Serial Bus (USB), which is connected to the monthly data logger, HOBO RX3000. The data obtained from stations over three years were classified yearly to analyze the characteristics of each parameter to detect climate variability within AHFR.

Water Level Velocity Discharge Monitoring

Water level at the catchment outlet was monitored during high flow on an hourly basis from 13rd October 2016 to 16th October 2017 via a stage board (installed on 10 October 2016) with rising samplers at a height interval of 0.1 m starting from 0.4 m until 0.9 m. The HOBO MX2001 Pressure Transducer connected to a data logger

was installed inside a vertical pipe mounted at the catchment outlet on 1st February 2017 (see Figure 1b). Continuous (15 minutes interval) water level data were connected to a Samsung Galaxy S2 Tab Bluetooth, in which it recorded data every two weeks (from 1st February 2017 to 24th December 2017).

Water velocity was measured using a SEBA velocity current meter at all water levels from October 2016 to October 2017. The equipment used and accuracy of river characteristics parameters are displayed in Table 2. The data were plotted on a rating curve (see Figure 2) by applying the average velocity area method (Turnipseed & Sauer, 2010). The use of a polynomial equation was best suited with water flow prediction at AHFR. The flow at AHFR was estimated using the following equation: $Y = 5.8909 - 7.8412X + 2.6187X^2$, where Y = discharge in m^3/s and X = water level in m. The coefficient of determination $R^2 = 0.97$ was close to unity (1), which signified a low discrepancy

Table 2: Equipment and accuracy of river characteristics parameters

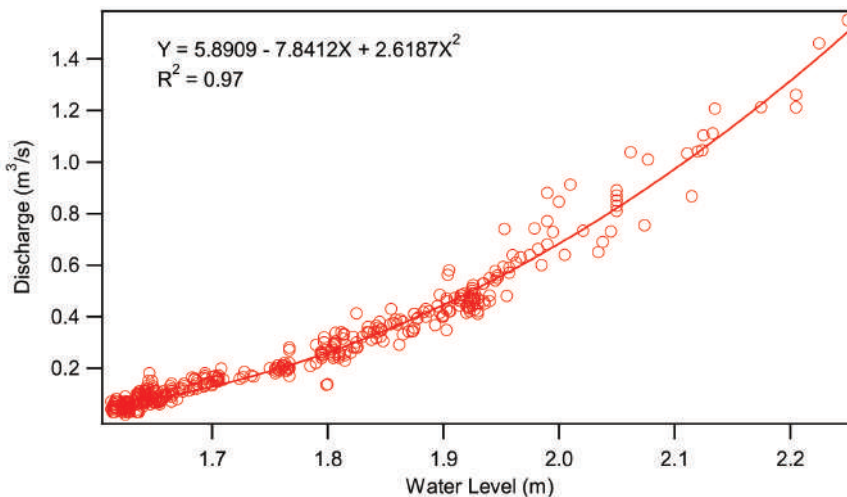| Parameters	Equipment	Accuracy
River width (m)	Meter tape	±1 to 50 m
River velocity (m/s)	SEBA velocity current meter	±0.01 s
River depth (m)	Staff gauge	±1 to 50 m

Figure 2: Discharge rating curve at the catchment outlet in the AHFR between October 2016 to October 2017

between the actual flow and the estimated flow. The flow estimation used a power, linear, and logarithmic equation, yielding an R^2 of 0.90, 0.92, and 0.90, respectively, all of which were lower than the polynomial equation.

Streamflow Quality Conditions

Stream water quality was analyzed during both baseflow and stormy conditions from 10 October 2016 to 16 October 2017 at the catchment outlet. The stream water was grab-sampled during baseflow conditions when it was not raining and during storm events for every 30 min. Storm events were sampled using a multi-stage sampler comprised of four 1-L plastic bottles tightened on a vertical mount at 0.1 m intervals (Figure 1b). The stream water was preserved in a cool box and stored in a refrigerator (< 4°C). Table 3 shows the analyses for dissolved oxygen (DO), pH, electric conductivity (EC), temperature,

salinity, total dissolved solids (TDS), turbidity, and total suspended solids (TSS) conducted by following the standard method to examine water and wastewater (APHA, 1915). A total of 28 stormy events occurred, with 262 samples collected during the study period. Suspended solids were one of the parameters defined as particles that were unable to pass through a filter, instead, leaving them suspended in the water. Meanwhile, suspended solids absorbed heat from sunlight and the temperature of the stream had increased (Yusoff *et al.*, 2019). Furthermore, dissolved oxygen level had decreased due to warmer water holding less oxygen than cooling water. Therefore, in such a scenario, a water body can lose its ability to support aquatic life diversity (Yahyapour & Golshan, 2014; Yusoff *et al.*, 2019). Since the activity of aquatic organism relies on DO, suitable pH is required to ensure sustainability.

Table 3: Selected water quality parameters, units, analytical methods, instruments, and accuracy following the standard method to examine water and wastewater

Parameter	Unit	Method	Instrument	Model/Type	Accuracy
Dissolved Oxygen	mg/L	In-situ measurement	DO meter	YSI200 DO meter	±1.5%
pH	pH		pH and temperature meter	YSI60 pH and Temperature	±0.02
Electric Conductivity	μs/cm		Electric conductivity/ temperature/ salinity/TDS	YS1300 EC meter	±1 μs/cm
Temperature	°C	Temperature field method			±0.15°C
Salinity	ppt	Electrical conductivity method			±2%
Total Dissolved Solids	mg/L	Total Dissolved Solids field method			±1%
Turbidity	Nephelometric Turbidity Unit	Nephelometric method	Turbidimeter	HACH 2100P	±0.01 NTU
Total Suspended Solids	mg/L	Gravimetric method	Temperature controlled oven/analytical balance/vacuum pump/filter paper	Millipore vacuum pump, Whatman filter paper sized 0.45 μm	±5 mg/L

Statistical Analysis

Three types of statistical analysis were performed to observe the behavioral pattern of water quality against the baseflow and stormflow events: Pearson correlation analysis, cluster analysis, and principal component analysis. Sinnakaudan *et al.* (2010) used the correlation coefficient to select the most influential parameters in an equation development. The Person coefficient of ±0.5 - ±1.0 indicates a high correlation, whereas ±0.3 - ±0.49 indicates a medium correlation, and ±0.10 - ±0.29 indicates a low correlation (Cohen, 2013). Cluster analysis was performed to group observations or variables into clusters based upon similarities (Everitt *et al.*, 2011). The clustering variables were the mean, minimum, and maximum values for the observed physicochemical properties at either the baseflow or stormflow events. The cluster analysis provided an estimation on whether or not the impacts of stormflow events were prominent for water quality status. The most prominent pollutant that affected water quality of the river system was checked via the principal component analysis. The Kaiser–Meyer–Olsen (KMO) measure of sampling adequacy should be greater than or equal to 0.6 to help determine the worthwhile of performing a principal component analysis on a set of variables (Sulaiman *et al.*, 2019).

Results and Discussion

Climate Variability in AHFR (2016–2017)

The total rainfall was 2382.73 mm for 2016 and 2041.41 mm for 2017. However, missing data were recorded from June 2017 to September 2017, which consequently affected the total rainfall for the year. The rainfall was comparable to MARDI and *Jabatan Pertanian* Serdang stations (Neto *et al.,* 2012). The wettest month was recorded in November 2017, with a total rainfall of 408.23 mm; whereas the driest month was observed in October 2016, with a total rainfall of 87.41 mm (Table 4). Within these two year data observations, November recorded the highest monthly rainfall, whereas June, July, and October recorded the lowest monthly rainfall.

The situation in forested area may have been attributable to the variation in terms of monthly rainfall compared with what was reported in Kuala Lumpur (Neto *et al.,* 2012). Air temperature ranged from 20.10°C to 37.90°C, with an average of 26.41°C from 1 January 2016 to 31 December 2017 (Figure 3). The warmest month was in April 2016, with a mean temperature of 28.09°C. The lowest temperature occurred in November 2017 with a mean of 25.72°C. The temperature was slightly higher than what was reported in a 1999 microclimate study that detailed an average temperature of 25.6°C and maximum of 27.7°C (Nuruddin & Awaluddin, 1999). Relative humidity differs from 77.2% to 100% with an average of 91.75% from 1st January 2017 to 31st December 2017.

Baseflow and Stormflow Discharge

Nearly 369 baseflow event ($n = 107$) and storm event ($n = 262$) samples were collected between 28 October 2016 to 16 October 2017 and their details are summarized in Table 5.

Storm events are classified into three classes based on the storm size: Light for rainfall less than 10 mm (17 events, 126 samples), medium for rainfall between 10–20 mm (6 events, 46 samples), and heavy for rainfall more than 20 mm (5 events, 51 samples). Baseflow discharge varied from 0.003 m³/s to 0.680 m³/s, whereas storm event discharge ranged from 0.010 m³/s to 1.090 m³/s. The percentage of baseflow to stormflow during storm events was 56.3%, which was comparable to other tropical catchments. Baseflow occurred most during the dry period (i.e., June, July, and October), whereas stormflow was the greatest during the wet period (November). The proportion of baseflow to stormflow depends on event size and lack of rain.

Streamflow Quality (10 October 2016 – 16 October 2017)

During baseflow and stormflow periods, the streamflow quality and characteristics (10 October 2016 to 16 October 2017) were analyzed, including the physicochemical quality

Table 4: Summary of rainfall analysis obtained from the weather station in the AHFR
from January 2016 – December 2017

Month-Year	Total Rainfall (mm)	Daily Maximum (mm)	Days with Rainfall > 70mm	Non-Rainfall Days
January 2016	254.04	80.82 (17 January 2016)	1	9
February 2016	110.62	46.01 (23 February 2016)	0	14
March 2016	251.86	46.01 (25 March 2016)	0	11
April 2016	106.81	28.41 (30 April 2016)	0	17
May 2016	339.64	40.21 (2 May 2016)	0	7
June 2016	137.21	43.80 (17 June 2016)	0	20
July 2016	162.04	37.61 (16 July 2016)	0	16
August 2016	103.61	47.01 (30 August 2016)	0	19
September 2016	186.42	47.21 (01 September 2016)	0	14
October 2016	87.41	38.41 (7 October 2016)	0	14
November 2016	320.24	55.42 (26 November 2016)	0	3
December 2016	322.83	78.819 (26 December 2016)	1	10
January 2017	329.63	66.41 (23 January 2017)	0	8
February 2017	250.42	55.01 (25 February 2017)	0	13
March 2017	362.25	43.81 (5 March 2017)	0	6
April 2017	296.02	35.4 (20 April 2017)	0	6
May 2017	150.63	39.01 (30 May 2017)	0	11
June 2017	N/A	N/A	N/A	N/A
July 2017	N/A	N/A	N/A	N/A
August 2017	N/A	N/A	N/A	N/A
September 2017	N/A	N/A	N/A	N/A
October 2017	113.61	21.61 (29 October 2017)	0	16
November 2017	408.23	61.21 (22 November 2017)	0	4
December 2017	107.42	31.81 (19 December 2017)	0	12

both for baseflow (n = 107) and stormflow (n = 262) conditions, as shown in Table 6. The baseflow event (m³/s) ranged from 0.003 (8 November 2016) to 0.680 (21 April 2017), whereas ~~for~~ the stormflow event ranged from 0.010 (9 November 2016) to 1.090 (7 March 2017). High rainfall intensities (> 20 mm/h, n = 5 events) led to peak discharges recorded at 0.500, 0.894, and 1.013 m³/s, respectively. This phenomenon significantly recharged the post-event baseflow discharges at 0.169, 0.561, and 0.627 m³/s, respectively.

According to the National Water Quality Standards (NWQS), water quality status falls under Class I during baseflow event. Class I indicates practically no treatment for the water supply (Department of Environment DOE, 2004). The EC of 27.70 μS/cm < 1000 μS/cm, TDS of 17.84 mg/L < 500 mg/L, turbidity of 1.35 NTU < 5.0 NTU, DO of 8.67 mg/L > 7.0 mg/L, and TSS of 8.33 mg/L < 25.0 mg/L signified Class I status. The water quality status during stormflow event remained in Class I. The average EC, TDS, turbidity, DO, and TSS were 28.02 μS/cm, 18.15 mg/L, 4.22 NTU, 9.06 mg/L, and 9.46 mg/L, respectively. The
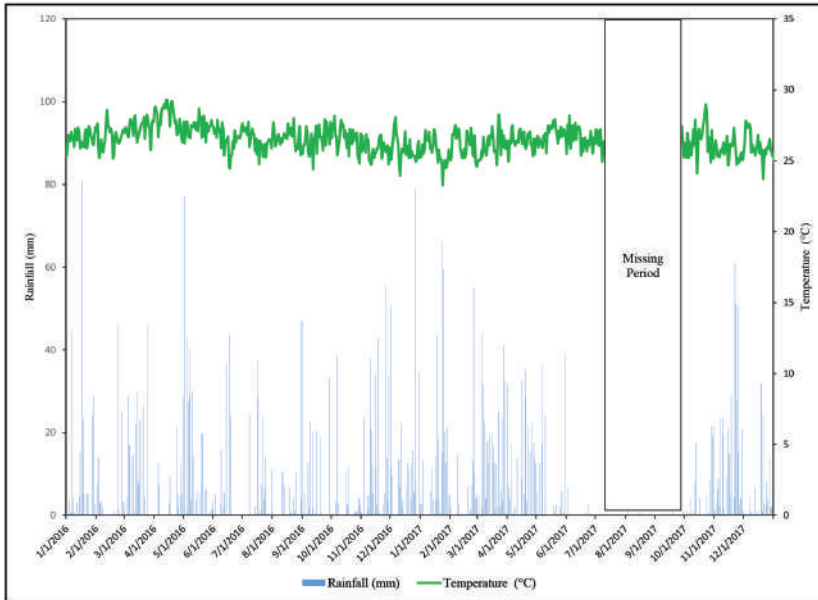
Figure 3: Daily rainfall and average temperature in the AHFR from January 2016 to December 2017

Table 5: Summary of baseflow data in the AHFR from 28 October 2016 to 16 October 2017

Date	Duration (hr)	Rainfall Intensity (mm/h)	No. of Samples			Total Discharge, Q_{total} (m³/s)	Minimum Discharge, Q_{min} (m³/s)	Peak Discharge, Q_{peak} (m³/s)	Antecedent Rainfall (day)
			Light (i < 10 mm/h)	Medium (11 < i > 20 mm/h)	Heavy (i > 20 mm/h)				
28 October 2016	2	0.6	7			0.100	0.020	0.020	0
29 October 2016	3	4.2	16			1.337	0.020	0.142	0
30 October 2016	1	4.2	16			0.448	0.029	0.044	0
09 November 2016	1.5	1	16			0.271	0.010	0.026	0
10 November 2016	0.5	20.2			17	3.894	0.007	0.527	0
11 November 2016	1.7	20.4			14	2.626	0.140	0.500	0
21 February 2017	0.6	0.4	8			1.545	0.249	0.266	0
23 February 2017	0.5	7.2	7			1.901	0.246	0.583	0
24 February 2017	1.5	2.8	10			2.387	0.263	0.266	0
07 March 2017	0.7	14.8		8		4.930	0.450	1.090	0

Date									
08 March 2017	0.7	19.8		6		2.375	0.493	0.646	0
09 March 2017	0.7	4	5			1.494	0.498	0.498	0
16 March 2017	1	15.6		5		1.801	0.317	0.450	2
17 March 2017	0.7	14.6		6		2.351	0.339	0.535	0
20 March 2017	2	2.8		10		4.826	0.529	0.539	0
24 March 2017	2	1.8	11			6.094	0.535	0.573	0
03 April 2017	1.7	4.4	10			7.353	0.672	0.749	0
06 April 2017	0.2	0.2	8			3.195	0.527	0.539	0
07 April 2017	0.5	0.6	8			4.031	0.488	0.520	0
18 April 2017	2	3.8	6			2.665	0.428	0.450	0
19 April 2017	0.5	25.01			7	5.182	0.859	0.894	0
20 April 2017	0.5	34.8			7	5.284	0.552	1.013	0
02 May 2017	1	5.2	6			3.131	0.517	0.537	0
06 May 2017	0.5	36.21			6	3.874	0.380	0.853	0
18 May 2017	0.5	2.2	10			3.347	0.312	0.346	7
13 October 2017	4	17.4		11		1.645	0.092	0.213	0
16 October 2017	0.2	2.4	8			0.929	0.044	0.160	1

Table 6: Streamflow qualities and quantities during baseflow and stormflow conditions
(10 October 2016 – 16 October 2017)

	Baseflow ($n = 107$)			Stormflow ($n = 262$)		
	Mean	**Min**	**Max (Date)**	**Mean**	**Min**	**Max (Date)**
Q (m³/s)	0.281	0.003	0.680 (21 April 2017)	0.327	0.010	1.090 (7 March 2017)
DO (mg/L)	8.67	6.15	12.59 (8 February 2017)	9.06	7.50	11.80 (10 November 2016)
pH	4.84	3.14	8.58 (7 February 2017)	4.80	3.28	6.43 (30 October 2016)
Temperature (°C)	25.48	23.00	26.70 (16 May 2017)	25.28	23.40	26.40 (18 May 2017)
Salinity (ppt)	0.00	0.00	0.00	0.01	0.00	0.80 (8 March 2017)
EC (µS/cm)	27.70	14.30	72.10 (10 March 2017)	28.02	14.20	151.70 (8 March 2017)
TDS (mg/L)	17.84	9.30	46.20 (10 March 2017)	18.15	9.30	97.30 (8 March 2017)
TSS (mg/L)	8.33	1.00	8.5 (12 November 2016)	9.46	1.00	57.00 (20 April 2017)
Turbidity (NTU)	1.30	0.70	7.10 (12 November 2016)	4.22	0.67	37.70 (11 November 2016)

pH values for baseflow and stormflow events were 4.84 and 4.80, respectively, both of which are under Class IV. The water quality status in Class IV was suitable for irrigation but not for drinking water.

The behavior of the physicochemical parameters during the stormflow with different intensities Figures 4 a - c. The behavior of EC, TSS, and turbidity showed slight changes during the stormflow, in which the EC values remained in Class I, while both TSS and turbidity values changed into that of Class II. According to the NWQS, the Class I conditions of freshwater for TSS and turbidity were about 25 and 5 mg/L, respectively. The highest value during the stormflow for TSS was 57 mg/L on 20 April 2017, with a rainfall intensity of 36.40 mm/h. The turbidity was 37.70 NTU on 11 November 2016 with a rainfall intensity of 20.40 mm/h.

A thunderstorm that occurred on 8th March 2017 might have resulted in the dramatic increments of the EC, salinity, and TDS values, which were 48.1 - 151.7 µS/cm, 0 - 0.8 ppt, and 31 - 86.4 mg/L, respectively. For freshwater from forest catchment area, normally, the salinity value is 0 ppt. On the day of the thunderstorm, only these three parameters showed abnormal increases (Figure 4b). However, these parameters were still considered to be in good conditions even with these high values, which meant it was safe for the water to be in contact with the body. In this experimental catchment, these parameters rarely reached these high readings, thus making it a very interesting future topic to study. Specifically, future studies should examine the relationship of these parameters and how they change, especially during thunderstorms.
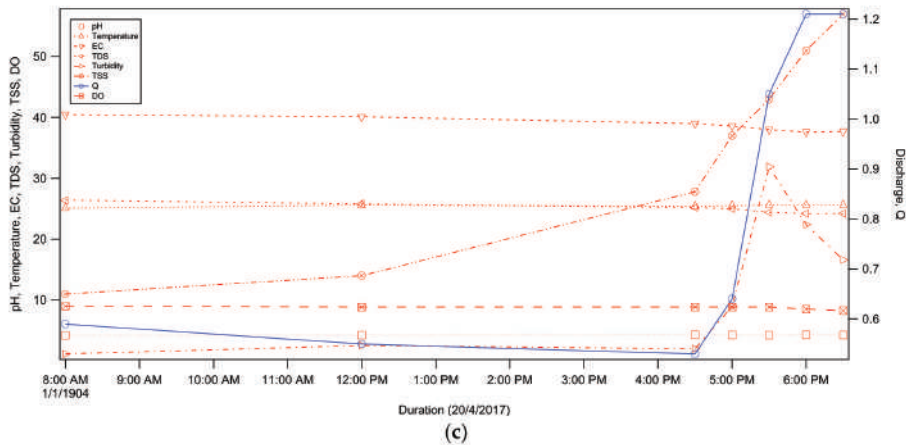

(a)

(b)
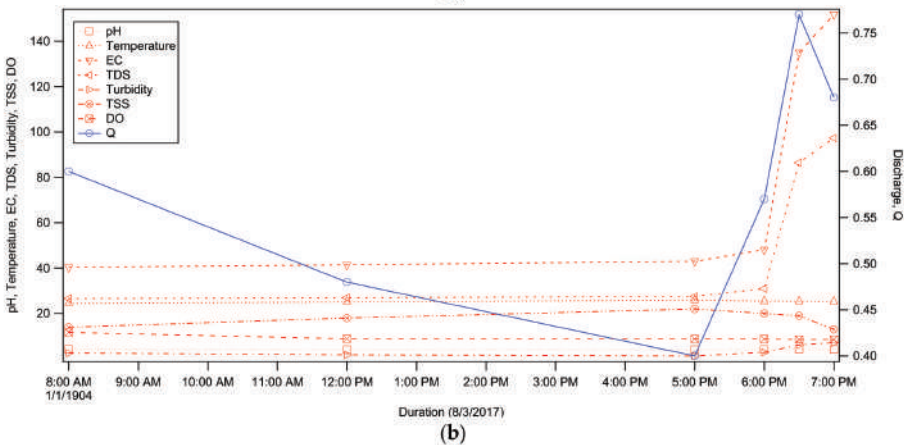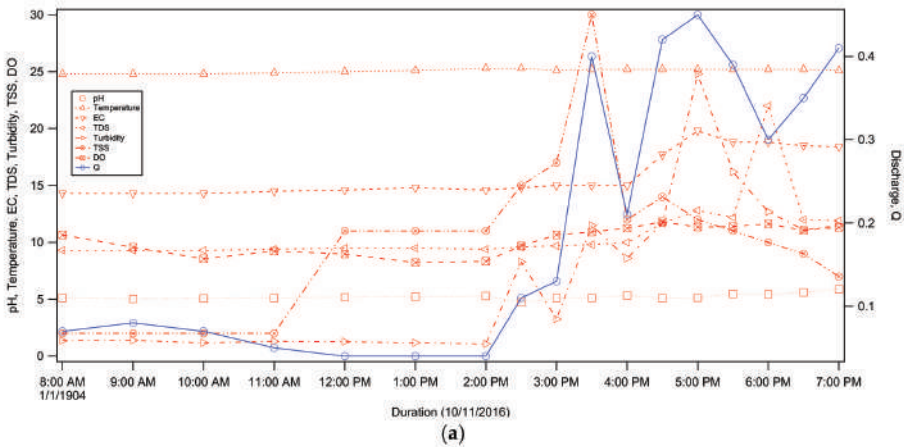
Figure 4: Pollutograph of a storm event on: (a) 10 November 2016; (b) 8 March 2017; and (c) 20 April 2017, which characterized the trend of discharge and water quality parameter in AHFR

The results of this work indicated that the stream water catchment has high water quality during both baseflow and stormflow events, except for pH values. The presence of igneous rock is rich in quartz and granite, contributing to a lower pH for both baseflow and stormflow events. Aizat *et al.* (2013) described igneous rock as a common acidic soil that may contribute to lower pH values. The highest value for TSS during stormflow events was 57 mg/L on 20 April 2017, where the associated rainfall intensity was 36.40 mm/h. The presence of high TSS during stormflow events is evident in Figures 5a - b. High TSS in a river system was an indication of suspended fine particles in the water column. The unidirectional flow of the river system transport suspended particles further downstream from the observation area. The computation of suspended sediment load transport was inferred from Syuhada *et al.* (2018). The maximum discharge measured during baseflow was 0.680 m^3/s. Furthermore, the stormflow was 1.090 m^3/s, while the associated TSS concentrations were 32 mg/L and 57 mg/L, respectively (see Table 6). The maximum suspended sediment load reached 0.0218 kg/s and 0.0621 kg/s during baseflow and stormflow events, respectively. These values were higher, especially during stormflow, considering the presence of coarse particles in the river system. The coarse particles at river bottom may induce the settling of fine particles due to the trapping and filtering mechanism (Sulaiman *et al.*, 2017). Thus, an extensive study was encouraged to obtain more information pertaining to erosion and sedimentation along the longitudinal profile of the river system.

Behavior of Water Quality during Baseflow and Stormflow Events

Baseflow and stormflow events can be differentiated by either rainfall or non-rainfall days during the sampling execution. It is believed that storm events induce a greater chance of soil detachment, and thus, more suspended pollutants can be expected at the river system. Table 7 depicts analysis on stormflow and baseflow water quality data, which revealed inconsistent variations. The measures of central tendency, variability, and shape for water quality variables depicted the departure from normal distribution. Of particular interest, the standardized skewness and standardized kurtosis statistics showed values of outside the range of −2 to +2 for the majority of the observed variables, indicating a significant departure from normality.

Figure 5: Upper Rasau river catchment outlet during: (a) baseflow; and (b) stormflow conditions

Table 7: Summary statistics of water quality during baseflow and stormflow events

Baseflow Event								
	Conductivity	Discharge	DO	pH	TDS	Temperature	TSS	Turbidity
Count	119	119	119	119	119	119	119	119
Average	26.3756	0.248259	8.70941	4.86319	16.9874	25.4857	7.64706	1.30504
Standard deviation	11.6557	0.218361	0.969211	0.793992	7.55275	0.565279	7.11836	0.741968
Coefficient of variation	44.1912%	87.9568%	11.1283%	16.3266%	44.4609%	2.21802%	93.0862%	56.854%
Minimum	14.3	0.02	6.15	3.28	9.3	23.0	1.0	0.7
Maximum	72.1	1.4	12.59	7.58	46.2	26.7	41.0	7.1
Range	57.8	1.38	6.44	4.3	36.9	3.7	40.0	6.4
Standardized skewness	5.8824	8.73111	1.75814	6.14679	6.07671	−3.02508	11.5742	20.2118
Standardized kurtosis	6.68439	13.828	5.61786	5.37012	7.13958	5.16321	15.8117	69.6109
Stormflow Event								
	Conductivity	Discharge	DO	pH	TDS	Temperature	TSS	Turbidity
Count	51	51	51	51	51	51	51	51
Average	25.9745	0.441176	9.86235	5.18902	17.0392	25.1529	17.1137	9.68961
Standard deviation	8.59686	0.361107	1.32771	0.64446	5.50988	0.407113	15.5724	7.9506
Coefficient of variation	33.0973%	81.851%	13.4624%	12.4197%	32.3365%	1.61855%	90.9936%	82.0528%
Minimum	14.3	0.04	8.06	4.22	9.3	24.2	2.0	0.85
Maximum	40.5	1.21	11.8	6.1	26.4	25.8	57.0	37.7
Range	26.2	1.17	3.74	1.88	17.1	1.6	55.0	36.85
Standardized skewness	0.300312	2.62434	0.161071	−1.14781	−0.0141841	−0.831747	2.82161	4.27572
Standardized kurtosis	−1.91969	−0.525891	−2.58939	−1.9322	−1.90618	−0.706512	−0.5922	4.17972

Since the variable distributions were not normal, a non-parametric test was performed to compare the medians rather than the means of observed variables. Non-parametric tests do not assume that data come from normal distributions and tend to be less affected by outliers (Hair *et al.*, 2006). The Mann–Whitney (Wilcoxon) W statistic test was used to conclude the medians of two populations: The baseflow and stormflow variables. The Mann–Whitney (Wilcoxon) W-test was used to compare medians of two populations with a null hypothesis of median1 = median2, while an alternative hypothesis was determined to be median1 ≠ median2. The non-parametric test for all variables in Table 8 rejected the null hypothesis, thus accepting the alternative hypothesis that the median value for all variables during a baseflow event differed to the median variable values during a stormflow event. The quantile plot in Figure 6 verified the distinct differences of water quality variables during baseflow and stormflow events. If the samples are collected from the same population, the quantile plot should be close together. The offset between baseflow and stormflow plots indicated a difference between them. An alteration in the slope of the curves designate a difference between the standard deviations. The offsets were visible at the upper tail, signifying variations at higher values. Therefore, water quality for both the baseflow and stormflow events were significantly different in the AHFR. It is generally known that water quality during baseflow and stormflow events are dissimilar, a detailed analysis was performed using a multivariate approach (correlation, cluster, and principal component analysis). Statistical methods offer a means of performing the analysis in an objective way to eliminate the common confusion of conflicting subjective opinions. They are capable of distinguishing between randomness (e.g., noise, random variability) and patterns (e.g., seasonality, trend) using repeatable procedures. Because of the role of chance in each measurement, statistical methods call for a water quality variable to be viewed as a stochastic process. While a random variable does not imply some natural ordering

of the results, a stochastic variable does (e.g., a time series of data at a particular site, or a set of samples down a river at the same time).

The correlation analysis was separately performed for baseflow data and stormflow data. The water discharge was crucial in determining the pH level, temperature, conductivity, TDS, turbidity, TSS, and DO. Increasing and decreasing water discharge determined the fate of the aforementioned water quality parameters. Figure 7a shows the Pearson correlation coefficient for baseflow data, while Figure 7b shows it for stormflow data. It is evident that the increased amount of discharged water from the baseflow to stormflow significantly influenced the increase of TSS. The correlation coefficient significantly increased from a medium correlation (0.49) to a high correlation (0.9), as opposed to others. It was elucidated that the TSS level in the AHFR was proportionally related to water discharge. Variations in TSS concentration in rivers during storms often resulted in a hysteresis effect (Chow *et al.*, 2017). Three forms of hysteresis loops were proposed in the past: Clockwise, anticlockwise, and that which is shown in Figure 8 (Seeger *et al.*, 2004). The direction of the hysteresis loop indicates the concentration of TSS during either the rising or falling limb of a hydrograph (House & Warwick, 1998; Bowes *et al.*, 2005; Lloyd *et al.*, 2016; Chow *et al.*, 2017), while the slope of a hysteresis loop infers the mechanical denudation of either initial erosion, late erosion, or sediment deposition (Ndam Ngoupayou *et al.*, 2016). The hysteresis loop of TSS in Figure 8 reveals the anticlockwise pattern, which depicts a higher TSS concentration during a falling limb of a rainfall hydrograph. The soil detachment in the AHFR is delayed due to the presence of vegetative cover at the majority of catchment areas. The initial erosion, late erosion, and sediment deposition phase occurred during July–December, April–May, and January–March, respectively. Cluster analysis was performed by clustering the event into mean, minimum, and maximum for baseflow and stormflow conditions, respectively. The dendrogram plot in Figure 9 indicates that each case formed

different clusters. It showed that different cases contributed to different behavioral patterns. The first clusters were those containing a mean baseflow and mean stormflow at a distance of 0.2, wherein the baseflow and stormflow joined into a single cluster containing a mean baseflow and stormflow. At the third step, maximum baseflow joined the previous clusters. The maximum stormflow formed a unique cluster and differed from previous clusters. It can be concluded that two main groups exist: the first group is up from the mean baseflow to maximum baseflow, while the second group is the maximum stormflow. The second group is prevalent due to the significant increase of in quality values, as depicted in Table 8. The factorability test of the principal component analysis depends on KMO values. The KMO value (0.70) for stormflow data was larger than 0.16, which indicated a worthwhile PCA performance. The scree plot in Figure 10a is helpful in determining the number of principal components to extract: 2. The biplot that contained loading and weight for each water quality and its associate component is shown in Figure 10b. Conductivity, pH, TDS, temperature, and TSS corresponded with variables in Component 1, while turbidity and DO correspond to Component 2. The strong weight and loading of turbidity at Component 2 in Table 8 has been proven to be a prominent and visible pollutant in the AHFR.
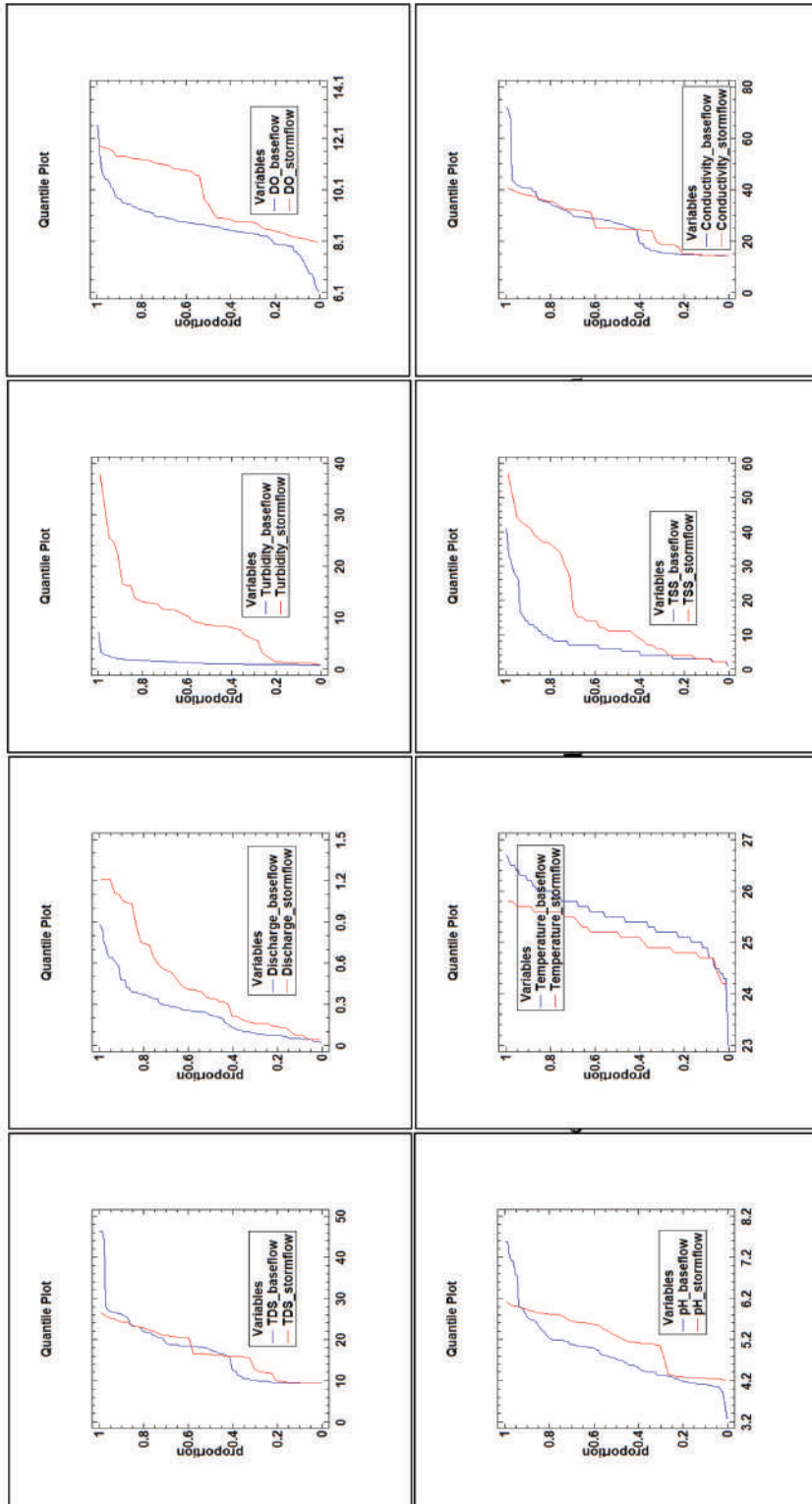
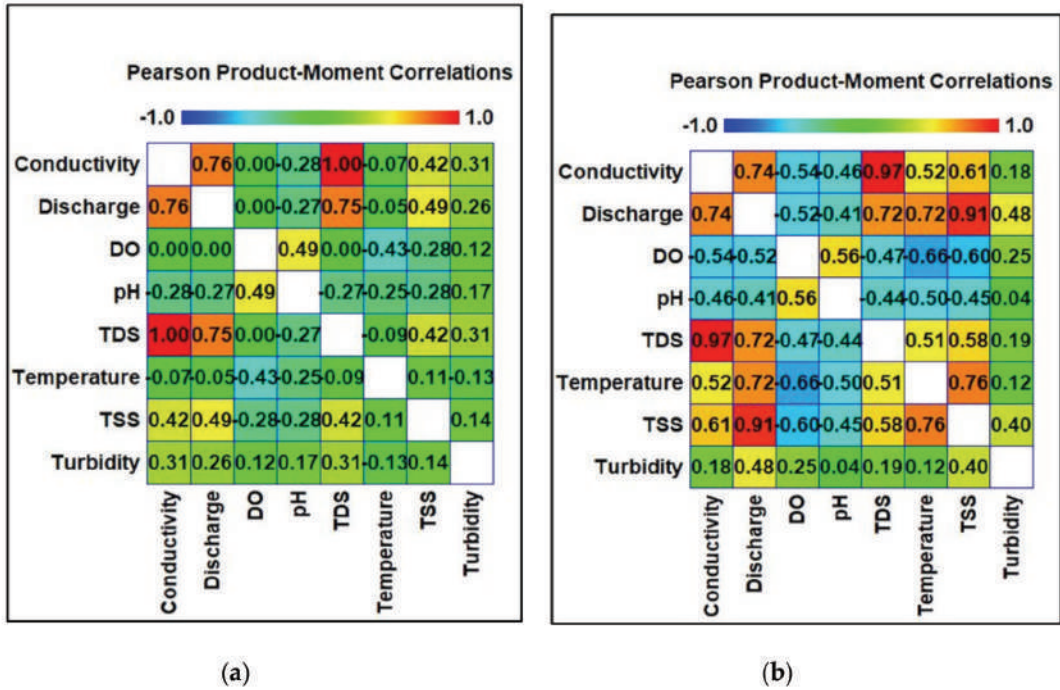Figure 6: Quantile plot for observed water quality in the AHFR during baseflow and stormflow events

Figure 7: Pearson correlation coefficient during: (a) baseflow; and (b) stormflow conditions
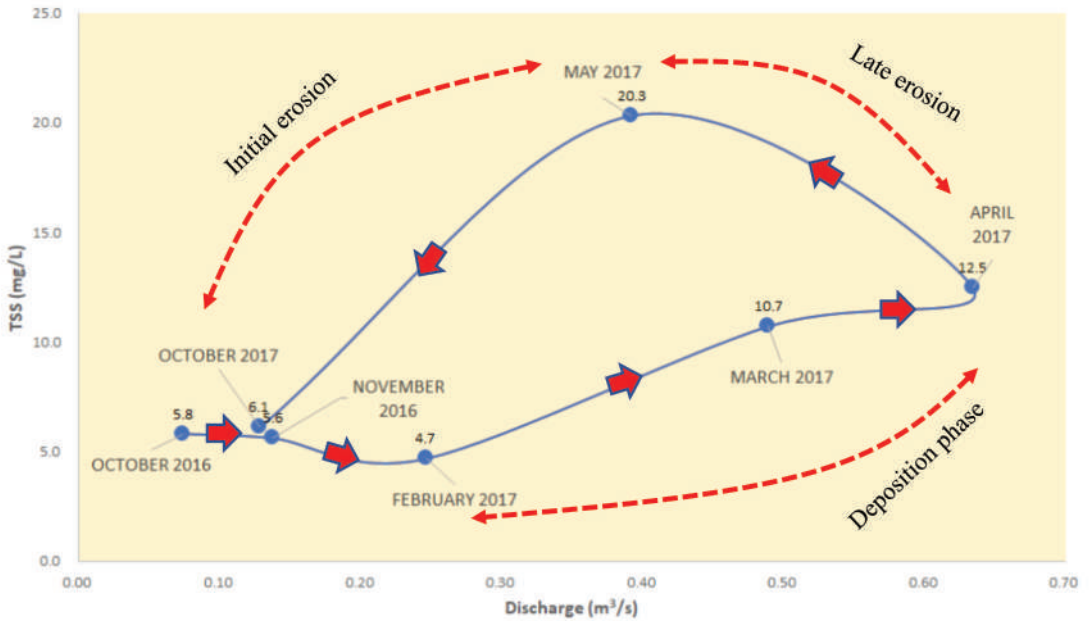

Figure 8: Anti-clockwise hysteresis loop of TSS in the AFHR
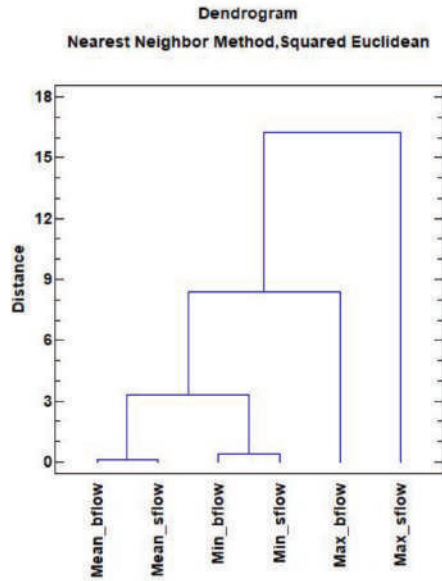
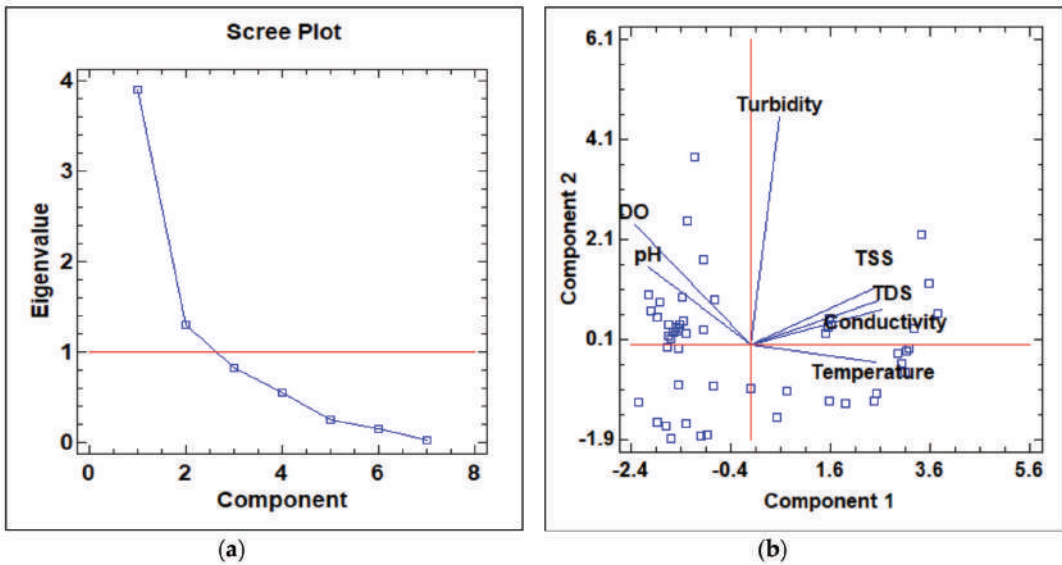Figure 9: Dendrogram plot for factor analysis

Figure 10: (a) Scree plot; and (b) biplot for principal component analysis

Table 8: Component weights for principal component analysis

Parameters	Component 1	Component 2
Conductivity	0.43556	0.125445
DO	−0.388623	0.426127
pH	−0.34203	0.274897
TDS	0.423138	0.154231
Temperature	0.41383	−0.0622293
TSS	0.428076	0.209916
Turbidity	0.0934065	0.809559

Conclusion

The acquisition of hydrological data in the form of rainfall, streamflow, and water quality parameters are crucial for AFHR due to the lack of databases at the current stage. This study was initiated to assess seasonal physicochemical characteristics from a matured secondary forest catchment for water quality status. The seasonal pattern was defined as either baseflow or stormflow events in the AFHR. The majority of stormflow events were considered as light events, where the bulk of rainfall intensity occurred < 10 mm/h. The flow rating curve was best suited when using the polynomial equation $R^2 = 0.97$. The non-parametric test revealed that median water quality values during baseflow events were different than during stormflow events. By using the Mann–Whitney (Wilcoxon) W-test, it was evident that the null hypothesis of the same median values was rejected, and thus, the alternative hypothesis of the different median values is accepted. These findings signify that although AFHR is a forest land, rainfall erosivity is able to introduce pollutants at different rates and intensities, especially when compared to the baseflow event. The TSS is believed to have a high correlation against river discharge with a Pearson coefficient of 0.91 during storm events. The significant change of TSS was dominant compared with other parameters during storm events. Although the turbidity and TSS did not correspond to the same component, both parameters were dominant pollutants in the AFHR, with strong loading on each respective component. Low correlation between TSS and turbidity was observed as the turbidity was mostly caused by organic materials in the water. TDS and conductivity had higher correlation coefficient against water discharge, as portrayed in Figure 7. The component loadings were almost identical to the TSS, signifying the importance of TDS and conductivity diffusion in the AHFR. Extensive data collection is still required in this study area in order to provide information on flow variation and its quality within an isolated tropical forest catchment. While this study does not offer a conclusive answer to the question of "what is the main pollutant source in the AHFR?", it does provide a proven analysis that the variation of flows exhibited different behavioral pattern in the AHFR.

Acknowledgements

References

Aizat, M., Roslan, M., & Sulaiman, W. (2013). Water quality index of selected station at Rasau river, Ayer Hitam forest reserve, Puchong, Selangor. *J. Water Resour., 1*, 37-42.

APHA. (1915). *Standard methods for the examination of water and wastewater* (Vol. 2). American Public Health Association.

Bawon, P. (2007). *Ayer Hitam forest reserve: Multimedia super corridor community heritage*. Serdang, Selangor: UPM.

Bowes, M. J., House, W. A., Hodgkinson, R. A., & Leach, D. V. (2005). Phosphorus-discharge hysteresis during storm events along a river catchment: The River Swale, UK. *Water Research, 39*(5), 751-762.

Canadell, J. G., Le Quéré, C., Raupach, M. R., Field, C. B., Buitenhuis, E. T., Ciais, P., . . . Marland, G. (2007). Contributions to accelerating atmospheric CO2 growth from economic activity, carbon intensity, and efficiency of natural sinks. *Proceedings of the National Academy of Sciences, 104*(47), 18866-18870.

Ceola, S., Laio, F., & Montanari, A. (2015). Human pressure on rivers is increasing worldwide and threatens water security. *Proceedings of the International Association of Hydrological Sciences, 366*, 109.

Chow, M. F., Huang, J.-C., & Shiah, F.-K. (2017). Phosphorus dynamics along river continuum during typhoon storm events. *Water, 9*(7), 537.

Christina, M., Nouvellon, Y., Laclau, J. P., Stape, J. L., Bouillet, J. P., Lambais, G. R., & Le Maire, G. (2017). Importance of deep water uptake in tropical eucalypt forest. *Functional Ecology, 31*(2), 509-519.

Cohen, J. (2013). *Statistical Power Analysis for the Behavioral Sciences*. Taylor & Francis.

Deere, N. J., Guillera‐Arroita, G., Platts, P. J., Mitchell, S. L., Baking, E. L., Bernard, H., . . . Davies, Z. G. (2020). Implications of zero‐deforestation commitments: Forest quality and hunting pressure limit mammal persistence in fragmented tropical landscapes. *Conservation Letters, 13*(3), e12701.

Department of Environment DOE. (2004). *Environmental Quality Report 2004*. Kuala Lumpur: Department of Environment Malaysia. 179 Pages.

Department of Statistics Malaysia. (2005). *Malaysia Economic Statistics - Time Series*. Putrajaya: Department of Statistics.

Everitt, B. S., Landau, S., Leese, M., & Stahl, D. (2011). *Cluster analysis* (5th ed.). John Wiley.

Faizalhakim, A., Nurhidayu, S., & Norizah, K. (2017). Climate variability in relation with land use changes over a 30-year period in kelantan river basin. *The Malaysian Forester, 80*(1), 12-30.

Faridah-Hanum, I., & Rosly, Z. (2000). *Species composition of Ayer Hitam Forest, Puchong, Selangor.* Paper presented at the Proceedings of the 1999 Langat Basin Research Symposium.

Grimm, N. B., Faeth, S. H., Golubiewski, N. E., Redman, C. L., Wu, J., Bai, X., & Briggs, J. M. (2008). Global change and the ecology of cities. *Science, 319*(5864), 756-760.

Hair, J. F., Black, W. C., Babin, B. J., Anderson, R. E., & Tatham, R. L. (2006). *Multivariate data analysis* (6th ed.). Uppersaddle River: Pearson Prentice Hall.

Hasmadi, M., & AL, S. N. H. (2017). Estimated DEM uncertainty in creating a 3-D of the UPM's Ayer Hitam Forest reserve in Selangor, Malaysia. *Geografia-Malaysian Journal of Society and Space, 4*(1).

Houghton, R., & Hackler, J. (1999). Emissions of carbon from forestry and land-use change in tropical Asia. *Global Change Biology, 5*(4), 481-492.

House, W. A., & Warwick, M. S. (1998). Hysteresis of the solute concentration/discharge relationship in rivers during storms. *Water Research, 32*(8), 2279-2290.

Kanae, S., Oki, T., & Musiake, K. (2001). Impact of deforestation on regional precipitation over the Indochina Peninsula. *Journal of Hydrometeorology, 2*(1), 51-70.

Lai, F., & Samsuddin, M. (1985). Suspended and dissolved sediment concentrations of two disturbed lowland forested watersheds

in Air Hitam forest reserve, Selangor. *Pertanika*.

Laurance, W. F. (1999). Reflections on the tropical deforestation crisis. *Biological Conservation, 91*(2-3), 109-117.

Laurance, W. F. (2007). Forest destruction in tropical Asia. *Current Science*, 1544-1550.

Laurance, W. F., Goosem, M., & Laurance, S. G. (2009). Impacts of roads and linear clearings on tropical forests. *Trends in Ecology & Evolution, 24*(12), 659-669.

Lawson, T. (2015). The nature of the firm and peculiarities of the corporation. *Cambridge Journal of Economics, 39*(1), 1-32.

Lloyd, C., Freer, J., Johnes, P., & Collins, A. (2016). Using hysteresis analysis of high-resolution water quality monitoring data, including uncertainty, to infer controls on nutrient and sediment transfer in catchments. *Science of The Total Environment, 543*, 388-404.

Mabuchi, K., Sato, Y., & Kida, H. (2005). Climatic impact of vegetation change in the Asian tropical region. Part I: Case of the Northern Hemisphere summer. *Journal of Climate, 18*(3), 410-428.

Malhi, Y., & Grace, J. (2000). Tropical forests and atmospheric carbon dioxide. *Trends in Ecology & Evolution, 15*(8), 332-337.

Malhi, Y., & Wright, J. (2004). Spatial patterns and recent trends in the climate of tropical rainforest regions. *Philosophical Transactions of the Royal Society of London. Series B: Biological Sciences, 359*(1443), 311-329.

Morante-Filho, J. C., Arroyo-Rodríguez, V., de Andrade, E. R., Santos, B. A., Cazetta, E., & Faria, D. (2018). Compensatory dynamics maintain bird phylogenetic diversity in fragmented tropical landscapes. *Journal of Applied Ecology, 55*(1), 256-266.

Ndam Ngoupayou, J., Dzana, J., Kpoumie, A., Ghogomu, R. T., Fouepe Takounjou, A., Braun, J.-J., & Ekodeck, G. (2016). Present-day sediment dynamics of the Sanaga catchment (Cameroon): From the total suspended sediment (TSS) to erosion balance. *Hydrological Sciences Journal, 61*(6), 1080-1093.

Neto, V., Ainuddin, N. A., Wong, M., & Ting, H. (2012). Contributions of forest biomass and organic matter to above-and belowground carbon contents at Ayer Hitam Forest Reserve, Malaysia. *Journal of Tropical Forest Science*, 217-230.

Norizah, K., Hasmadi, I., & Misnah, E. (2014). *Remote sensing and GIS application in best harvest management planning in Sultan Idris Shah Forestry Education Centre (SISFEC), UPM.* Paper presented at the IOP Conference Series: Earth and Environmental Science.

Nuruddin, A. A., & Awaluddin, S. (1999). Microclimate of Ayer Hitam Forest, Selangor. *Pertanika J. Trop. Agric. Sci, 22*(2), 125-129.

Peter, G. (2000). *The World's Water 2000-2001*. Washington DC: Island Press.

Rahim, A. A., & Shahwahid, H. M. (2009). Determinants of deforestation in Peninsular Malaysia: An ARDL approach. *The Malaysian Forester, 72*(2), 19-28.

Seeger, M., Errea, M.-P., Begueιa, S., Arnáez, J., Martι, C., & Garcιa-Ruiz, J. (2004). Catchment soil moisture and rainfall characteristics as determinant factors for discharge/suspended sediment hysteretic loops in a small headwater catchment in the Spanish Pyrenees. *Journal of Hydrology, 288*(3-4), 299-311.

Sinnakaudan, S. K., Sulaiman, M. S., & Teoh, S. H. (2010). Total bed material load equation for high gradient rivers. *Journal of Hydro-environment Research, 4*(3), 243-251. doi:https://doi.org/10.1016/j.jher.2010.04.018

Sodhi, N. S., Liow, L., & Bazzaz, F. (2004). Avian extinctions from tropical and subtropical forests. *Annu. Rev. Ecol. Evol. Syst., 35*, 323-345.

Sulaiman, M. S., Abood, M. M., Sinnakaudan, S. K., Shukor, M. R., Goh, Q. Y., & Chung, X. Z. (2019). Assessing and solving multicollinearity in Sediment Transport Prediction Models using Principal Component Analysis. *ISH Journal of Hydraulic Engineering*, 10.1080/09715010.09712019.01653799. doi:10.1080/09715010.2019.1653799

Sulaiman, M. S., Sinnakaudan, S. K., Azhari, N. N., & Abidin, R. Z. (2017). Behavioral of sediment transport at lowland and mountainous rivers: A special reference to selected Malaysian rivers. *Environmental Earth Sciences, 76*(7), 300. doi:10.1007/s12665-017-6620-y

Syuhada, N., Nurhİdayu, S., & Sofiyan, M. (2018). The effects of forest disturbance on lakes and reservoirs capacity in malaysia. *The Malaysian Forester, 81*(1), 73-99.

Turnipseed, D. P., & Sauer, V. B. (2010). *Discharge measurements at gaging stations* (3-A8). Retrieved from Reston, VA: http://pubs.er.usgs.gov/publication/tm3A8

United Nations. (2011). *World urbanization prospects: The 2005 revision*: United Nations Publications.

Werth, D., & Avissar, R. (2005). The local and global effects of Southeast Asian deforestation. *Geophysical Research Letters, 32*(20).

Wong, I. (1970). *Reconnaissance soil survey of Selangor*. Kuala Lumpur: Ministry of Agriculture and Lands.

Xiao-Jun, W., Jian-Yun, Z., Shamsuddin, S., Shou-Hai, B., Rui-Min, H., & Xu, Z. (2015). Assessing water security and adaptation measures in a changing environment. *Proceedings of the International Association of Hydrological Sciences, 366*, 129.

Yahyapour, S., & Golshan, A. (2014). Removal of total suspended solids and turbidity within experimental vegetated channel: Optimization through response surface methodology. *Journal of Hydro-environment Research, 8*(3), 260-269.

Yang, B., Wen, X., & Sun, X. (2015). Seasonal variations in depth of water uptake for a subtropical coniferous plantation subjected to drought in an East Asian monsoon region. *Agricultural and Forest Meteorology, 201*, 218-228.

Yusoff, M. K., Mohamed, K. N., Ismail, M. Z., Johan, S., & Hashim, N. H. M. (2019). Physico-chemical assessment of water resources in Pulau Pangkor, Perak, Peninsular Malaysia. *The Malaysian Forester, 82*, 17-26.